(23) C. Sandmark and C. Brändén, *Acta Chem. Scand.*, **21**, 993 (1967).
(24) D. M. L. Goodgame, M. Goodgame, P. J. Hayward, and G. W. Rayner-Canham, *Inorg. Chem.*, **7**, 2447 (1968).
(25) H. Sigel, B. E. Fischer, and B. Prijs, *J. Am. Chem. Soc.*, **99**, 4489 (1977).
(26) N. E. Dixon, C. Gazzola, R. L. Blakley, and B. Zerner, *Science*, **191**, 1144 (1976).
(27) R. C. Rosenberg, C. A. Root, and H. B. Gray, *J. Am. Chem. Soc.*, **97**, 21 (1975).
(28) F. A. Quiocho and W. N. Lipscomb, *Adv. Protein Chem.*, **25**, 1 (1971); W. N. Lipscomb, *Chem. Soc. Rev.*, **1**, 319 (1972).
(29) A. S. Brill and J. H. Venable, *J. Am. Chem. Soc.*, **89**, 3622 (1968).
(30) T. Blundell, G. Dodson, D. Hodgekin, and D. Mercola, *Adv. Protein Chem.*, **26**, 279 (1972).
(31) The overall stepwise formation constants are expressed here as the product of two terms; a "statistical" term and an "intrinsic" formation constant expressed in exponential form. The statistical factor depends upon the assumed number of equivalent coordination sites available to the incoming ligand. Thus, in the equilibrium $ML_i + L \rightleftarrows ML_{i+1}$ if M has four equivalent coordination sites there are $4 - i$ sites available to an incoming ligand and $i + 1$ sites from which a ligand can dissociate. Thus, the formation of ML_{i+1} is biased by a purely probabilistic or "statistical" factor of $(4 - i)/(i + 1)$. If one assumes six equivalent coordination sites the statistical factor is $(6 - i)/(i + 1)$. Dividing the overall formation constant by the statistical factor yields the so-called "intrinsic" formation constant which is a measure of the binding strength for a single coordination site in the species ML_i. For a more detailed description of this kind of treatment see ref 32.
(32) A. R. Burkin, *Q. Rev., Chem. Soc.*, **5**, 1 (1951).

Contribution from Ames Laboratory—U.S. Department of Energy, Iowa State University, Ames, Iowa 50011

Synthesis and Characterization of New Metal–Metal Bonded Species. 3. Dimeric Tantalum(III) Halide Adducts with Tetrahydrothiophene. Characterization of Structure-Bonding Features through NQR Spectroscopy

J. L. TEMPLETON and R. E. McCARLEY*

Received December 29, 1977

The synthesis of the first tantalum(III) halide adducts $Ta_2X_6(SC_4H_8)_3$ (X = Cl, Br) is described. Properties of these diamagnetic dimers are related to the known metal–metal bonded confacial bioctahedral structure which consists of two halogen atoms and the sulfur of one tetrahydrothiophene ligand bridging between the two metal atoms with two halogen atoms plus one tetrahydrothiophene bound as terminal ligands on each metal. The ^1H NMR, infrared, and UV–visible spectra all correlate well with the important structural features. NQR spectra are reported for the halogen nuclei as well as for ^{93}Nb in the homologous series of crystalline derivatives $Nb_2X_6(SC_4H_8)_3$ (X = Cl, Br, I) and $Ta_2X_6(SC_4H_8)_3$ (X = Cl, Br). In the structurally characterized bromides the ^{81}Br spectra correlate fully with the known unit cell symmetry; in these cases four resonances at lower frequency and two at higher frequency are definitively assigned to the terminal and bridging bromine atoms of the dimer, respectively. Strong π back-bonding from halogen to metal results in lower resonance frequencies for the terminal halogen atoms as compared to the frequencies of the bridging atoms in all cases. The ^{93}Nb NQR coupling constants of the three niobium dimers increase in the order Cl < Br < I. This order is consistent with a nearly constant contribution from d electrons involved in metal–metal bonding to the niobium NQR and decreasing contribution from d electrons involved in metal–ligand bonding to the net ^{93}Nb electric field gradient.

Introduction

There are still broad gaps in our knowledge concerning chemistry of the lower oxidation state halide complexes of niobium and tantalum.[1] In particular, there is an absence of information regarding well-characterized tantalum(III) halide complexes. The trihalides of tantalum are nonstoichiometric exhibiting compositions from $TaX_{2.9}$ to $TaX_{3.1}$.[2] The insolubility and lack of reactivity which characterize the trihalides make them unacceptable for synthetic manipulations directed toward derivatives of tantalum(III).

The descriptive chemistry of tantalum is dominated by the pentavalent complexes which constitute the majority of compounds reported to date.[3] The tetrahalides of tantalum are well characterized, and quadrivalent derivatives have been examined in recent years.[4] No trivalent halide complexes of tantalum have been confirmed in the literature. Blight, Deutscher, and Kepert reported that the reaction of $TaCl_4$ and acetonitrile led to the formation of $[TaCl_3(CH_3CN)_2]_2$,[5] which formally appears to correspond to tantalum(III). More recently McCarley and co-workers communicated the crystal structure of $\{[(C_6H_5)_3P]_2N\}_2\{Nb_2Cl_8(CH_3CN)_2C_4H_6N_2\}$ after a thorough investigation of the chemistry of niobium and tantalum tetrahalides in acetonitrile led to the above salt in order to elucidate the redox chemistry involved in these systems.[6] The culmination of the investigation was the identification of a unique bridging ligand revealed by the structure which resulted from the reductive coupling of two acetonitrile molecules and was accompanied by oxidation of the niobium to the 5+ oxidation state. It seems probable that the dimeric species isolated from earlier tantalum tetrachloride reactions with acetonitrile is a similar ligand-bridged complex of tantalum(V).

Previous work in this laboratory provided the new compounds of niobium(III) $Nb_2X_6(SC_4H_8)_3$ with X = Cl, Br, or I.[7] Since niobium is more easily reduced than tantalum and discrete halide complexes of tantalum(III) were unknown, the synthesis and characterization of molecular tantalum halide adducts of the form $Ta_2X_6(SC_4H_8)_3$ with X = Cl or Br were undertaken. In this report are described the synthetic route which led to isolation of the first tantalum(III) halide adduct with tetrahydrothiophene and the physical studies of these complexes. The complete crystal and molecular structure analysis of $Nb_2Br_6(SC_4H_8)_2$ and $Ta_2Br_6(SC_4H_8)_3$ reported previously[8] has shown that the compounds exist as molecular dimers with a confacial octahedral configuration[9] whereby the metal atoms are bridged by two bromine atoms and the sulfur atom of one tetrahydrothiophene ligand.

Experimental Section

The tantalum halides of interest in this study were all air and moisture sensitive. Manipulations of solids were therefore performed in a nitrogen-filled drybox and standard vacuum line techniques were employed for solvent transfers. Tantalum pentahalides were prepared

0020-1669/78/1317-2293$01.00/0

according to published procedures.[10] Tetrahydrothiophene was dried over lithium aluminum hydride and stored over the drying agent in a round-bottom flask equipped with a Teflon high-vacuum stopcock. Toluene was dried over molten sodium and distilled prior to use.

Tantalum was determined gravimetrically as the oxide, Ta_2O_5, after hydrolysis in aqueous ammonia and oxidation with nitric acid. Halides were determined by potentiometric titration using standardized silver nitrate solution. Carbon and hydrogen analyses were performed by the Ames Laboratory Analytical Service Group.

Tantalum(III) Halide Complexes. $Ta_2X_6(SC_4H_8)_3$. Sodium amalgam was prepared in an evacuated vessel by dropwise addition of 241 g of mercury/g of sodium. The amalgamation process is very exothermic, but after an initial induction period and a small flash the reaction proceeds smoothly with no danger of excessive heat generation.

In a typical preparation $TaCl_5$ (3.6 g, 10 mmol) was weighed into a 100-mL reaction flask with a Teflon-coated stirbar in the drybox. Sodium amalgam (110 g, 20 mmol) corresponding to a 2 to 1 mole ratio of sodium to tantalum was funneled into a side-arm bulb. The side-arm bulb was then inserted into the receptacle joint of the reaction flask prior to removal from the drybox. After the flask was attached to the vacuum line and after outgassing was done for 30 min, approximately 50 mL of dry toluene was condensed into the flask using a liquid nitrogen cooling bath. If the system was allowed to warm to room temperature, a pale yellow solution resulted from dissolution of some $TaCl_5$. Dry tetrahydrothiophene was next distilled under vacuum into a calibrated cylinder to ensure excess ligand. Distillation of the cyclic sulfide (3 mL, 35 mmol) into the reaction vessel led to the formation of a bright orange solution as the tetrahydrothiophene–tantalum pentachloride adduct formed almost instantaneously. Addition of the reducing agent was initiated by rotating the sodium amalgam filled side arm while vigorously agitating the solution with the magnetic stir bar. The amalgam was added over a period of several minutes and a series of color changes ensued. After 30 min the reaction was complete as indicated by a dark plum colored solution. Volatile components, mainly toluene and excess ligand, were removed from the heterogeneous reaction mixture by vacuum evaporation. The remaining material was removed from the flask in the drybox where grinding led to coalescence of the mercury which could then be decanted away from the solid. The solid products were then transferred to an extractor suitable for high-vacuum usage. Fresh toluene was effective in solubilizing the desired product and continuous extraction effected a clean separation of $Ta_2Cl_6(SC_4H_8)_3$ from the by-products. Slow solvent evaporation from the extractor deposited tris(tetrahydrothiophene)hexachloroditantalum as dark red-violet crystals. The analogous blue-violet bromide derivative was isolated via a similar procedure. Anal. Calcd for $Ta_2Cl_6(SC_4H_8)_3$: Ta, 43.13; Cl, 25.34; C, 17.18; H, 2.88. Found: Ta, 42.49; Cl, 24.80; C, 17.04; H, 3.16. Calcd for $Ta_2Br_6(SC_4H_8)_3$: Ta, 32.73; Br, 43.35; C, 13.03; H, 2.19. Found: Ta, 33.21; Br, 42.33; C, 13.15; H, 2.44.

Physical Measurements. Proton magnetic resonance spectra were obtained with either a Varian A-60 or a Hitachi Perkin-Elmer R-20B spectrometer. The crystalline material was loaded in the drybox into a specially designed cell equipped with a sintered glass frit and adapted for vacuum line use. Appropriate amounts of solvent and tetramethylsilane were then distilled into the cell prior to filtration and sealing of the NMR tube under vacuum. Solution electronic spectra were obtained using a Cary Model 14 recording spectrophotometer and an evacuable cell similar to that used for the preparation of NMR samples. By careful weighing of the cell after addition of the solid in the drybox and the solvent via distillation the concentration of the solution could be estimated when all of the solid dissolved. The extinction coefficients of low-intensity bands could then be calculated and successive dilutions allowed the remaining extinction coefficients to be computed by intensity comparisons with the previously characterized bands by utilizing a Beer's law assumption. The Faraday balance used to measure magnetic susceptibilities has been described.[11] Infrared spectra were obtained as Nujol mulls with NaCl plates (600–4000 cm^{-1}) on a Beckman IR-7 or IR-12 and polyethylene windows (100-700 cm^{-1}) on a Beckman IR-11 spectrophotometer. Nuclear quadrupole resonance spectra were obtained with a Wilk's NQR-1A superregenerative spectrometer as described by Edwards.[12] More accurate frequency measurements in the region of 5–50 MHz were possible with the wide line induction spectrometer designed by Torgeson.[13] Samples were transferred to 15 mm o.d. tubes in the drybox and sealed in vacuo.

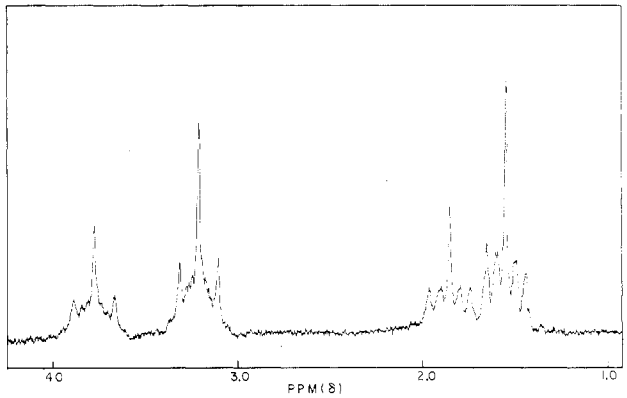

Figure 1. ^1H NMR spectrum of a saturated solution of $Ta_2Cl_6(SC_4H_8)_3$ in benzene.

Table I. Proton Magnetic Resonance Data for $Ta_2X_6(SC_4H_8)_3$[a]

assignment	δ[b] X = Cl	δ[b] X = Br	rel intens
type "α", terminal	1.39	1.39	2
	1.45	1.45	
	1.51	1.50	
	1.54	1.55	
	1.60	1.60	
type "α", bridging	1.69	1.86	1
	1.75	1.91	
	1.80	1.98	
	1.85	2.03	
	1.91	2.09	
type "β", terminal	3.09	3.19	2
	3.21	3.30	
	3.30	3.41	
type "β", bridging	3.65	4.02	1
	3.77	4.11	
	3.88	4.23	

[a] Spectra obtained from saturated benzene solution at ambient temperatures. [b] Chemical shifts are relative to Me_4Si in ppm.

Results and Discussion

Syntheses. Previous work had shown that preparation and isolation of $NbX_4(SC_4H_8)_2$ (where X = Cl, Br, or I) furnished suitable niobium(IV) species for a one-electron reduction with a sodium amalgam reducing agent. The solubility of the niobium(IV) adducts in benzene made possible the heterogeneous reduction across the amalgam–solution interface with the resultant production of the dimeric niobium species, $Nb_2X_6(SC_4H_8)_3$.[7] The complete absence of any discrete tantalum(III) halide species endowed the analogous tantalum system with considerable chemical merit. Unfortunately, the intractable products resulting from the interaction of tantalum(IV) halides with thioethers precluded isolation of $TaX_4(SC_4H_8)_2$, and thus a one-electron route to tantalum(III) was not available. In addition, it was known that the anhydrous trihalides of tantalum were unreactive and unsuitable for starting materials in the preparation of molecular tantalum(III) compounds.

The synthetic approach employed to prepare tantalum(III) derivatives was simple and direct. The reactants were the soluble mono(tetrahydrothiophene) adduct of tantalum pentahalide and 2 mol of sodium/mol of tantalum. In anticipation of a tetrahydrothiophene to metal ratio of 1.5 to 1.0 in the desired product, excess ligand was added to ensure the availability of the cyclic sulfide for coordination during the reduction. A series of color changes following addition of the amalgam indicated that reduction was proceeding through several intermediate species. Precipitation of sodium halide occurred as a consequence of sodium oxidation and halide ion

abstraction, and these observations in conjunction with the intensely colored aromatic solution were consistent with the formation of a soluble reduced tantalum compound. The solubility of the reduced species made it amenable to purification via extraction, and analytical data were consistent with the formulation $Ta_2X_6(SC_4H_8)_3$. Yields of 75% were typical for the isolation of purified chloride and bromide dimeric products.

Proton Magnetic Resonance Spectra. The ^1H NMR of neat tetrahydrothiophene exhibits two areas of resonance corresponding to the methylene protons adjacent to the heteroatom (labeled type α for purpose of discussion) and protons on the methylene groups further removed from the sulfur atom (type β). The type β resonance is in the form of an inexact quintet at δ 1.87 (relative to Me_4Si at δ 0) and the type α proton resonance appears as a skewed triplet at δ 2.74. Benzene solutions show similar splitting patterns with the chemical shifts at δ 1.47 and 2.54 for type β and α, respectively. The ^1H NMR spectrum of $Ta_2Cl_6(SC_4H_8)_3$ in benzene revealed four multiplets due to coordinated tetrahydrothiophene in the complex as shown in Figure 1. Two crude triplets were present at low fields with an integrated intensity ratio of 1 to 2 and two upfield quintets displayed the same intensity ratio. None of the observed resonances were attributable to free tetrahydrothiophene, and the conclusion reached was that tetrahydrothiophene was present in the molecular species in two different environments in a ratio of 2 to 1. The above ^1H NMR data are in accord with the known structure consisting of a confacial bioctahedral dimer[9] in which one tetrahydrothiophene serves as a bridging ligand while two are terminally coordinated to opposite metal atoms as in the analogous niobium dimers.

The observed downfield shift of the bridging tetrahydrothiophene resonances is consistent with an inductive effect removing electron density from the methylene protons as the sulfur lone pair electrons are donated into metal–ligand bonds. The formation of two dative bonds from the bridging ligand would remove more electron density than the single bond formed by the terminal sulfides. Thus the lower chemical shift of the bridging ligand type α protons as compared to the terminal ligand type α protons can be satisfactorily explained. The clear separation of the upfield quintets in $Ta_2Cl_6(SC_4H_8)_3$ is somewhat unexpected in view of the distal location of the type β methylene protons relative to the metal–sulfur interaction. The resolution of these two quintets in the tantalum dimer can be contrasted with the overlapping multiplet present in the niobium ^1H NMR spectrum.[7] The ^1H NMR data lead to the conclusion that the type β methylene protons of the bridging tetrahydrothiophene communicate more intimately with the sulfur–metal dative bonds in the tantalum case than in the niobium case. No firm theoretical basis for this behavior has been established. The relevant proton magnetic resonance data are summarized in Table I.

Electronic Absorption Spectra. Band maxima and extinction coefficients characterizing the electronic spectra of $Ta_2Cl_6(SC_4H_8)_3$ and $Ta_2Br_6(SC_4H_8)_3$ in benzene solution are listed in Table II as well as the corresponding data for $Nb_2Cl_6(SC_4H_8)_3$ and $Nb_2Br_6(SC_4H_8)_3$ for comparative purposes.[7] The similarity among the four spectra is quite striking, as would be expected if the transitions are centered mainly on the metal atoms and the gross electronic structure of all four is the same. The energy level separations show a clear trend in both tantalum and niobium to increase from bromide to chloride, in accord with the expected spectrochemical relationship between bromide and chloride, as well as exhibiting the expected tendency toward larger energy spacings for tantalum than for niobium.

The extinction coefficients show similar trends for corresponding bands in the niobium and tantalum derivatives; that is, they vary in tandem, but the absolute values differ greatly. The tantalum compounds exhibit corresponding extinction coefficients almost an order of magnitude larger than the niobium analogues. It seems likely that the increased value of the spin–orbit coupling constant for tantalum, a third-row transition metal, as compared to niobium, a member of the second row, must play an important role in determining the oscillator strength of these electronic transitions.

Table II. Electronic Absorption Band Parameters[a]

$Ta_2Cl_6(SC_4H_8)_3$		$Ta_2Br_6(SC_4H_8)_3$		$Nb_2Cl_6(SC_4H_8)_3$[b]		$Nb_2Br_6(SC_4H_8)_3$[b]	
$10^3\nu$, cm^{-1}	ϵ[c]	$10^3\nu$, cm^{-1}	ϵ[c]	$10^3\nu$, cm^{-1}	ϵ[c]	$10^3\nu$, cm^{-1}	ϵ[c]
9.5	17	8.5	22	9.1	3	8.0	3
11.0	29	9.6	28	11.5	5	10.5	8
14.8	300	13.6	320	13.1	8	11.9	11
20.5	4000	19.4	5300	18.4	430	17.4	600

[a] Spectra obtained in benzene solutions. [b] Data taken from ref 7. [c] Molar extinction coefficients are in units of $L\,mol^{-1}\,cm^{-1}$.

Table III. Magnetic Susceptibility Data[a]

compound	$10^6\chi_{app}$, emu/g	$10^6\chi_M$, emu/mol	$10^6\chi_D$, emu/mol	$10^6\chi_{cor}$, emu/mol
$Ta_2Cl_6(SC_4H_8)_3$	−0.33	−276	−371	+95
$Ta_2Br_6(SC_4H_8)_3$	−0.24	−254	−431	+177
$Nb_2Cl_6(SC_4H_8)_3$[b]	−0.28	−187	−380	+193

[a] Solid samples were used for susceptibility measurements at 25 °C. Abbreviations: χ_{app} = apparent susceptibility per gram; χ_M = molar susceptibility = molecular weight times apparent susceptibility; χ_D = calculated diamagnetic susceptibility per mole; χ_{cor} = corrected susceptibility = $\chi_M - \chi_D$. [b] Data taken from ref 7.

The magnitude of the extinction coefficients deserve comment. For a monomeric octahedral complex, the Laporte forbidden bands typically have extinction coefficients on the order of 10 L mol^{-1} cm^{-1} and bands that are also spin forbidden are found to be perhaps 100 times less intense. The smallest extinction coefficient observed in the dimeric tantalum species reported here is 17 L mol^{-1} cm^{-1} and the values range upward to 5300 L mol^{-1} cm^{-1} for the band at 19.4×10^3 cm^{-1} in $Ta_2Br_6(SC_4H_8)_3$. This range of intense absorptions is consistent with a strong metal–metal interaction which destroys the applicability of simple monomeric selection rules. Effective overlap of the metal d orbitals to form molecular orbitals would by their parentage encompass the highest occupied molecular orbital and lowest unoccupied molecular orbital, and thus electronic transitions would occur within this arena. Incorporation of atomic orbitals from both metal atoms into molecular orbitals eliminates the monomeric intensity restrictions and the result is more intense absorption bands.

Magnetic Susceptibility. The Faraday method was utilized to determine the susceptibilities of the two tantalum dimers at 25 °C and the results are listed in Table III where data for $Nb_2Cl_6(SC_4H_8)_3$ are listed for comparison. The observation of well-resolved nuclear magnetic resonance spectra indicated the absence of paramagnetic species, and indeed the bulk susceptibility measurements confirmed that the dimers were diamagnetic.

A diamagnetic correction factor based on Pascal's constants was applied to the observed susceptibility,[14] and the resultant was a small paramagnetic contribution. This small positive susceptibility was similar to that of $Nb_2Cl_6(SC_4H_8)_3$ as determined by a temperature-dependence study.[7] By analogy with the niobium case this value of the corrected susceptibility may be attributed to temperature-independent paramagnetism. This interpretation is consistent with a diamagnetic ground state in which all of the electrons are paired while an admixture of excited states introduces a small amount of paramagnetism.

Table IV. Tetrahydrothiophene Infrared Frequencies (700–1400 cm^{-1})[a]

SC_4H_8 (in CS_2)[b]	$Ta_2Cl_6(SC_4H_8)_3$	$Ta_2Br_6(SC_4H_8)_3$	$Nb_2Cl_6(SC_4H_8)_3$[c]	$Nb_2Br_6(SC_4H_8)_3$	$NbCl_4(SC_4H_8)_2$[b]
		800 s, sh			801 m
816 m	809 s	810 s	810 s	806 m-s	
					872 m
882 s	883 s	881 s	886 s	882 s	881 m
	956 s	958 s	959 s	958 m-s	960 m
	967 m	968 s	964 s		
996 s		999 vw			
		1023 w	1027 w-m, sh	1021 w	1025 w
1035 w-m	1039 m	1038 m	1041 m	1037 w-m	1038 w
1060 w-m		1060 vw			
	1075 m	1073 m		1072 w-m	1075 w-m
	1082 w	1082 w	1083 m	1082 w	
1129 w-m	1126 s	1127 s	1129 s	1125 m-s	1128 w-m
	1128 s	1132 s, sh			
		1189 w, sh	1194 w-m, sh		
1197	1200 m	1199 m	1203 m	1200 w	1193 w
1215 w, sh	1214 w	1211 m	1214 m	1211 w-m	1214 w-m
			1248 m, sh		
1256 s	1257 s	1255 s	1256 s	1252 m	1254 m
	1268 s	1268 s	1270 m-s	1267 m	1267 w-m
1308 w-m	1307 s	1306 s	1308 s	1306 s	1308 w-m
	1322 w	1320 w	1326 w		
		1329 w		1330 vw	

[a] Spectra obtained from Nujol mulls unless otherwise noted. Abbreviations: s, strong; m, moderate; w, weak; sh, shoulder. [b] Reference 24. [c] Reference 25.

The corrected susceptibility values are small in magnitude and therefore have fairly large relative errors associated with them, but nonetheless the expected trends are observed. An inverse dependence on the energy-level separations is predicted by perturbation theory because the excited paramagnetic state contribution to the ground state is inversely proportional to the energy difference between the two states. Chloride ion typically exhibits greater ligand field strength than bromide, and third-row transition metals are known to undergo larger energy splitting than their first- or second-row counterparts. The measured susceptibilities and calculated magnitudes of the temperature-independent paramagnetism (TIP) are consistent with these qualitative predictions: $Ta_2Cl_6(SC_4H_8)_3$ exhibits a smaller value for TIP than $Ta_2Br_6(SC_4H_8)_3$, and $Ta_2Cl_6(SC_4H_8)_3$ has a smaller value than $Nb_2Cl_6(SC_4H_8)_3$. The diamagnetic behavior of the tantalum dimers is consistent with the short Ta–Ta distance of 2.710 (2) Å found in $Ta_2Br_6(SC_4H_8)_3$[8] and the presence of a metal–metal double bond in which the four metal valence electrons are paired.

Infrared Spectra. The fingerprint region from 700 to 1400 cm^{-1} contains intraligand vibrations as evident in Table IV where absorptions for the two new tantalum dimers are listed along with data for other germane tetrahydrothiophene-containing complexes. The only absorptions above 1400 cm^{-1} were those near 3000 cm^{-1} due to C–H stretching modes. The conclusion drawn from these data is that tetrahydrothiophene is coordinated in a normal manner in these complexes. The term normal here is only meant to imply that the ligand retains its integrity while datively bonding via the sulfur electrons.

A second observation deals with the splitting of several infrared bands in the dimers as noted in comparing $Ta_2Br_6(SC_4H_8)_3$ and $Nb_2Br_6(SC_4H_8)_3$. The niobium spectrum exhibits four single bands which are split in the tantalum case. It may be that whatever factors displace the two type β quintets from one another in the ^1H NMR spectrum of the tantalum dimer also play a role in splitting the vibrational bands of the bridging and terminal ligands more clearly in the case of tantalum than niobium. Regardless, both the infrared and ^1H NMR data support the premise that the properties of bridging vs. terminal tetrahydrothiophene vary more within the tantalum dimer than in the niobium analogue.

Although spectral data in the low-frequency infrared region offer the possibility of information with regard to metal–ligand bond strengths, positive identification of these vibrational bands is difficult and interpretation of the data is therefore undertaken in light of these limitations. The low-frequency infrared data are listed in Table V.

Table V. Low-Frequency Infrared Data for $Ta_2Cl_6(SC_4H_8)_3$ and $Ta_2Br_6(SC_4H_8)_3$ (100–700 cm^{-1})[a]

$Ta_2Cl_6(SC_4H_8)_3$	$Ta_2Br_6(SC_4H_8)_3$
106 vw, vb	124 m
120 s	172 m
130 m, b	207 vs, sh
158 m	214 vvs
187 m, sharp	227 vs
204 w	238 s, sharp
213 w	331 m
226 m	477 w, b
242 vw, b	506 s, sharp
271 m	518 m
320 vvs	622 w
432 w, b	642 vw
476 w	663 m, sh
510 s, sharp	670 s
517 m, sh	
627 w, sh	
646 w, sh	
664 s, sh	
669 s	

[a] Spectra obtained from Nujol mulls unless otherwise noted. Abbreviations: s, strong; m, moderate; w, weak; v, very; sh, shoulder; b, broad.

The most definitive band assignment in this region is the C–S ring stretch which occurs at 683 cm^{-1} in the free tetrahydrothiophene molecule.[15] Upon coordination this band shifts to lower frequencies, typically located between 660 and 670 cm^{-1}.[16] A strong doublet is seen in both $Ta_2Cl_6(SC_4H_8)_3$ and $Ta_2Br_6(SC_4H_8)_3$ in this region; this splitting is presumably due to different C–S stretching frequencies for the bridging and terminal ligands. This C–S stretch is another example of splitting in the tantalum case which is absent in the niobium case, and thus further confirms the strong bridging tetrahydrothiophene bond to tantalum as compared to the corresponding niobium interaction.

Metal–halogen stretching bands are assigned in the region of 320 cm^{-1} for $Ta_2Cl_6(SC_4H_8)_3$ and 214 cm^{-1} for $Ta_2Br_6(SC_4H_8)_3$. The large dipole associated with these met-

Table VI. Halogen Nuclear Quadrupole Resonance Data[a] for $M_2X_6(SC_4H_8)_3$ Dimers (M = Nb, Ta; X = Cl, Br, I)

frequency, MHz	assignment	frequency, MHz	assignment
^{35}Cl in $Nb_2Cl_6(SC_4H_8)_3$		^{35}Cl in $Ta_2Cl_6(SC_4H_8)_3$	
8.547	terminal	9.230	terminal
8.603	terminal	9.286	terminal
8.613	terminal	9.356	terminal
8.981	terminal		
8.989	terminal		
		10.321	bridging
9.947	bridging	10.623	bridging
^{81}Br in $Nb_2Br_6(SC_4H_8)_3$		^{81}Br in $Ta_2Br_6(SC_4H_8)_3$	
59.11	terminal	62.78	terminal
59.48	terminal	63.22	terminal
59.70	terminal	63.83	terminal
60.86	terminal	64.70	terminal
67.35	bridging	71.47	bridging
69.85	bridging	73.94	bridging

^{127}I in $Nb_2I_6(SC_4H_8)_3$

ν_1,[b] MHz	ν_2,[c] MHz	η[d]	e^2Qq/h, MHz
Terminal Ligands			
90.61	152.4	0.393	522.7
90.75	155.6	0.367	533.0
94.95	157.9	0.407	542.5
Bridging Ligands			
120.7	195.2	0.443	673.8
121.3	196.9	0.438	679.3

[a] For spectra obtained at room temperature (25 °C). [b] Frequency of $M_I(1/2) \rightarrow M_I(3/2)$ transition. [c] Frequency of $M_I(3/2) \rightarrow M_I(5/2)$ transition. [d] Asymmetry parameter.

Table VII. Comparison of Halogen NQR Frequencies in Ta(III) and Ta(V) Compounds[a] (MHz)

compound	$Ta_2Cl_6(SC_4H_8)_3$	Ta_2Cl_{10}	$Ta_2Br_6(SC_4H_8)_3$	Ta_2Br_{10}
bridging	10.321	13.334	71.47	90.13
	10.623	13.356	73.94	90.32
		13.377		90.43
terminal	9.230	7.598	62.78	55.02
	9.286	7.641	63.22	55.15
	9.356	7.663	63.83	55.28
		8.141	64.70	56.19
		8.231		56.69
		8.261		56.96

[a] Data for Ta_2Cl_{10} and Ta_2Br_{10} taken from ref 19; ^{81}Br frequencies were calculated from ^{79}Br frequencies by the division factor 1.1971, $\nu_{^{81}Br} = \nu_{^{79}Br}/1.1971$.

al–halogen bonds absorbs infrared radiation very effectively, and hence the most intense bands in the low-energy portion of the spectra were assigned to metal–halogen vibrations. The tantalum(III) bromide derivative exhibits three strong bands in this region (207, 214, and 227 cm^{-1}) which can all be attributed to metal–bromine stretching modes since the confacial bioctahedral structure will conform to C_{2v} molecular symmetry which is sufficiently low that more than three of the metal–halogen normal modes are infrared active. In the chloride dimer, the band at 320 cm^{-1} is extremely broad and intense, but no shoulder or split bands are evident. The energy of a vibration theoretically changes as the square root of the inverse mass ratio, and in this case $M_{Br}^{1/2}/M_{Cl}^{1/2} = 1.5$ and 320 $cm^{-1}/214$ $cm^{-1} = 1.5$, so the frequency ratio is appropriate for a change in mass from chloride to bromide with retention of similar force constants.

Definitive vibrational analysis of the metal–sulfur vibrations for both terminal and bridging tetrahydrothiophene ligands is inappropriate in view of the limited data currently available.

Nuclear Quadrupole Resonance Spectra. Spectra of the halogen nuclei were obtained for both tantalum dimers and their previously prepared niobium analogues.[7] The resonance frequencies found for ^{35}Cl, ^{81}Br, and ^{127}I are listed in Table VI. Identification of the reported resonances for the chlorides and bromides was confirmed by location of the mated resonance, either ^{37}Cl or ^{79}Br, at the frequency dictated by the ratio of nuclear quadrupole moments, $Q(^{79}Br)/Q(^{81}Br) = 1.1971$ and $Q(^{35}Cl)/Q(^{37}Cl) = 1.2688$.[17]

A survey of the six resonances in both $Nb_2Br_6(SC_4H_8)_3$ and $Ta_2Br_6(SC_4H_8)_3$ clearly divides the absorptions into two types based on frequency differences. In each case, the four lowest frequencies span a range of 1.75–1.92 MHz and the two higher frequencies differ by 2.47–2.50 MHz, while a much larger gap of 6.49–6.77 MHz separates the two types. Based on the known crystal structure and confacial bioctahedral molecular configuration of these compounds, the two types of resonances can be unambiguously assigned to the terminal and bridging bromine atoms, respectively, for the low- and high-frequency types. In both compounds the unit cell contains two molecules related by a center of inversion, space group $P\bar{1}$. Thus the unit cell contains four terminal and two bridging bromine atoms which are crystallographically nonequivalent. The four low-frequency resonances correspond exactly to the four crystallographically independent terminal bromine atoms, and the two high-frequency resonances correspond to the two independent bridging bromine atoms.

The assignment of ^{35}Cl NQR resonances in $Nb_2Cl_6(SC_4H_8)_3$ and $Ta_2Cl_6(SC_4H_8)_3$ indicated in Table VI was made by analogy to the ^{81}Br spectra. However, in the ^{35}Cl spectra the multiplicities are not as neatly related to the molecular confacial bioctahedral structure, nor is the pattern of resonances the same for $Nb_2Cl_6(SC_4H_8)_3$ as for $Ta_2Cl_6(SC_4H_8)_3$. These data indicate that the crystal structures of the two chloride dimers are different from each other and also different from the structure of the bromide derivatives. That $Nb_2Cl_6(SC_4H_8)_3$ has a different crystal structure than $Nb_2Br_6(SC_4H_8)_3$ is confirmed by the ^{93}Nb NQR resonances given in Table VIII. The ^{93}Nb spectrum of $Nb_2Cl_6(SC_4H_8)_3$ shows that there are at least three nonequivalent Nb atoms per unit cell, whereas the ^{93}Nb spectrum of $Nb_2Br_6(SC_4H_8)_3$ conforms to the expected number of resonances for only two nonequivalent Nb atoms per unit cell as required by the space group $P\bar{1}$.

The relative positions of bridging and terminal halogen resonances may be considered in terms of the importance of π back-bonding from terminal halogen lone pair electrons into vacant d orbitals on the metal atom. Without question the assignment of ^{81}Br resonances is correct; i.e., the terminal bromine frequencies are lower than the bridging bromine frequencies. In contrast to what might be expected on a σ-only basis there has been a dramatic reversal in resonance frequencies such that the terminal bromines appear at lower frequencies than the bridging bromines. This assessment is based on considering the metal–terminal bromine bond distances are 0.10 Å shorter than the metal–bridging bromine distances, and in the group 3 metal halide dimers, e.g., Al_2Br_6, the terminal halides provide resonances at substantially higher frequencies than the bridging halides.[18] In the latter cases it is evident that the metal atoms (such as Al) are incapable of accepting electron density from the unshared electron pairs present on the terminal halogens since the four valence orbitals of the metal are all involved in σ-bonding interactions. Thus in the absence of π-bonding interactions it is clear that the terminal halogen resonances should appear at higher frequencies than those of the bridging atoms. These NQR data then rather unambiguously reflect a considerable contribution involving π bonding from halide to metal in the total metal–terminal halogen bonding scheme in these dimers.

The existence of π interactions has been documented for a series of hexahalometalates,[19] and the resonant frequencies

of halogens are found to reflect the extent of electron donation from the unshared halogen electron pairs to the metal. A qualitative description of the origins of the electric field gradient clarifies the balance between σ and π contributions. The molecular coupling constant, $|e^2Qq|_{mol}$, can be related to the atomic coupling constant, $|e^2Qq|_{atom}$, by an "unbalanced p" factor designated as U_p. For the axially symmetric case the major contribution to the halogen electric field gradient comes from the p-orbitals electron occupancy and is given by eq 1, where N is the electron occupancy of the orbital in question.

$$U_p = {}^1/_2(N_{px} + N_{py}) - N_{pz} \quad (1)$$

The role of U_p is illustrated by examining free chloride ion, where all three p orbitals are fully occupied and therefore $U_p = 0$, and then contrasting that value with diatomic chlorine where the occupancy of p_z is decreased to one electron as a result of the symmetrical covalent σ bond and hence $U_p = 1$. The experimental resonance frequency will thus vary from a theoretical value of zero for the spherically symmetrical Cl^- case to a value of 54.9 MHz for ^{35}Cl in the limiting case of a single nonpolar covalent σ bond. If only σ bonding were important any observed chlorine frequency would correlate directly with the bond polarity, but this is not the case. Since $|e^2Qq|_{mol}$ determines the nuclear quadrupole resonance frequency, it is the difference in $p\pi$ and $p\sigma$ as reflected in N_{pz}, N_{px}, and N_{py} which is crucial rather than the absolute magnitude of these components. Increased covalency in the metal–halogen σ bond causes an increase in the NQR frequency, but increased π bonding decreases the frequency. In the dimeric species reported here, the lower frequencies observed for the terminal halogens are probably attributable to increased π donation from these ligands while the bridging ligands are dominated by σ interactions only.

A contrasting dependence between σ- and π-electron donation from halide ions as a function of metal oxidation state is demonstrated nicely by comparison of the NQR results for tantalum(V) halide dimers[20] with the tantalum(III) dimers of this study. As the oxidation state of the metal increases, greater covalency is expected in the metal–halogen bonds. If only σ bonding is important, as is the case for bridging halides, a higher oxidation state metal will promote higher frequency absorptions than a lower oxidation state metal due to the increased covalency which effectively decreases N_{px} and N_{py} and thereby increases U_p.[21] An examination of the NQR data for bridging halogens in Table VII shows that such a variation occurs for tantalum(III) and -(V) halide bridges. The terminal resonances display the opposite behavior; the terminal resonant frequencies decrease as the oxidation state of the metal increases. Recognition of a significant π contribution in the terminal halide bonding to the metal offers a rational explanation for this apparent contradiction. Indeed N_{pz} will decrease as the metal is oxidized, but in addition N_{px} and N_{py} also will decrease as electron density is shared via the π interaction. If the total change in π donation exceeds the σ-donation change upon oxidation, then U_p will actually decrease, and this is evidently the case for the terminal halogens in $Ta_2X_6(SC_4H_8)_3$ and Ta_2X_{10} (X = Cl, Br).

Returning to the ^{93}Nb NQR spectra of the $Nb_2X_6(SC_4H_8)_3$ compounds, as listed in Table VIII, a few comments are required. First it is notable that the ^{93}Nb coupling constants deduced from the data are large, thus indicating a substantial electric field gradient at the metal atom. The electric field gradient arises primarily from two important structural features. Each metal atom in the dimers is surrounded by six ligands in a distorted octahedral array. This distorted octahedral symmetry is further reduced by the presence of two sulfur donors in each coordination sphere which are disposed trans to one another relative to each metal atom. Thus, there is a substantial tetragonal component to the electric field arising from the ligands which contributes to the net electric field gradient. The other important feature is the metal–metal bonding contribution to the net electric field gradient at the metal atom. The electric field gradient at the metal atom, for a transition metal, arises mainly from unbalanced electron population in the d orbitals[22] as reflected in the approximation

$$eq_{zz} = eq_{nlo}\{N(d_{z^2}) + {}^1/_2[N(d_{xz}) + N(d_{yz})] - [N(d_{xy}) + N(d_{x^2-y^2})]\}$$

Taking the metal–metal axis as an approximate threefold axis it is seen that the d_{z^2}, d_{xz}, and d_{yz} orbitals are involved mainly in the metal–metal bonding,[8] and the d_{xy}, $d_{x^2-y^2}$ orbitals mainly in metal–ligand bonding (along with the s and p orbitals). Because the signs of the appropriate d-orbital contributions are different in the equation above, the field gradient component arising from metal–metal bonding is opposed by the component arising from metal–ligand interactions. The average ^{93}Nb coupling constants of the three $Nb_2X_6(SC_4H_8)_3$ compounds clearly indicate that the magnitude of the net electric field gradient at the metal increases in the direction Cl < Br < I. This can tentatively be interpreted as a decreasing contribution from the metal–ligand bonding to the net electric field gradient since the metal–metal bonding contribution should remain relatively constant for the three compounds even though some lengthening of the Nb–Nb bond is expected in the order Cl < Br < I. In support of this argument it has previously been found that the ^{93}Nb and ^{181}Ta electric field gradients arising from halogen ligands in the M_2X_{10} (M = Nb, Ta; X = Cl, Br, I) compounds[23] do indeed decrease sharply in the order Cl > Br > I. Thus one can rationalize the observed halogen dependence by assuming the metal–metal bond contribution to the niobium electric field gradient is larger in magnitude than the metal–ligand bonding contribution of opposite sign and hence dominates the observed metal coupling constant. The halogen causing the largest contribution to the electric field gradient of the metal (Cl) then produces the smallest observed electric field gradient due to the subtractive nature of this component in the summation appropriate for these metal–metal bound dimers. Finally, the large electric field gradients, as reflected in the large ^{93}Nb

Table VIII. Nuclear Quadrupole Resonance Data for ^{93}Nb ($I = {}^9/_2$)

compound	frequencies, MHz $\nu_1({}^1/_2, {}^3/_2)$	$\nu_2({}^3/_2, {}^5/_2)$	$\nu_3({}^5/_2, {}^7/_2)$	$\nu_4({}^7/_2, {}^9/_2)$	η	e^2Qq/h, MHz
$Nb_2Cl_6(SC_4H_8)_3$	6.499	7.364	11.603	15.650	0.31	94.65
	6.389	6.940	10.951	14.810	0.34	89.72
	6.888	6.821	10.712	14.563	0.39	88.49
						90.95 av
$Nb_2Br_6(SC_4H_8)_3$		8.207	12.787	17.145	0.22	103.29
	6.156	7.808	12.244	16.452	0.26	99.26
						101.28 av
$Nb_2I_6(SC_4H_8)_3$		8.319	12.815	17.150	0.18	103.18
		8.487	12.834	17.124	0.08	102.80
						102.99 av

coupling constants, may be taken as another index of metal–metal bonding. In the only other cluster compound where strong metal–metal bonding is evident and the ^{93}Nb coupling constant has been determined, viz., in $[(CH_3)_4N]_2Nb_6Cl_{18}$, the electric field gradient was likewise very large.[13] Since the metal–metal bonding involves mainly interaction of d orbitals, the NQR coupling constants for metal atoms in cluster compounds should be enhanced in magnitude except in those cases where all five d orbitals participate nearly equally, as in the metal itself.

Conclusion

The two-electron reduction of tantalum pentahalide with sodium amalgam in the presence of excess tetrahydrothiophene proceeds smoothly to form the dimeric tantalum(III) halide adducts $Ta_2X_6(SC_4H_8)_3$ (X = Cl, Br). This paper presents the synthesis, spectral data, and magnetic behavior of the first tantalum(III) molecular halide complexes to be confirmed in the literature.

The ^1H NMR spectra are particularly informative based on analogy with the data obtained previously for $Nb_2X_6(SC_4H_8)_3$.[7] Assessment of one bridging tetrahydrothiophene and two terminal tetrahydrothiophene ligands via ^1H NMR correlate directly with the known confacial bioctahedral configuration[8] for $Ta_2X_6(SC_4H_8)_3$. The sharp ^1H NMR signals indicate the absence of paramagnetism, and susceptibility studies confirmed the diamagnetic behavior of the dimer. The presence of a tantalum–tantalum bond of order 2 offers a satisfactory explanation for the pairing of the four d electrons present in the dimeric molecule. Thus the condensation of monomeric tantalum units into a multiply bound metal–metal moiety has been effected during the synthesis.

Nuclear quadrupole resonance investigations complement the ^1H NMR data nicely. While ^1H NMR successfully probes the tetrahydrothiophene ligand environments and integration allows one to establish the ratio of bridging to terminal thioethers, NQR elucidates the environmental differences present for bridging and terminal halides. In the case of $Ta_2Br_6(SC_4H_8)_3$ and $Nb_2Br_6(SC_4H_8)_3$, the solid-state structure has one unique molecule per unit cell, and resolution of four terminal bromine absorptions and two bridging bromine absorptions not only confirms the presence of both bridging and terminal halides but also allows one to count the number of each type present in the molecule. Thus the successful application of NQR spectroscopy to an inorganic metal halide is ideally illustrated by the tantalum(III) bromide adduct reported here.

The opportunity to observe bridging and terminal halide NQR in dimers containing tantalum in the oxidation states 3+ and 5+ provides insight into the role of π bonding from lone pair electrons on the halogen atoms to vacant metal d orbitals. The relative importance of π bonding from halide to metal is much greater for terminal halides than for bridging halides. The donation of electrons into the σ framework is necessarily more for bridging halides forming bonds to two metal atoms than for terminal halides involved in only one σ bond to a metal atom. The decreased electron density on the halogen for bridging relative to terminal atoms is then reflected by decreased π donation of electron density to the metal by the bridging halides.

The isolation and characterization of tantalum(III) halide dimers with tetrahydrothiophene ligands promote further exploration of the chemistry of unusual oxidation states of this early transition metal by offering a convenient starting material for future investigations.

Acknowledgment. This work was supported by the U.S. Department of Energy, Office of Basic Energy Sciences, Materials Sciences Division. We are grateful to Patricia A. Finn for measurement of the ^{93}Nb NQR spectra.

Registry No. $Ta_2Cl_6(SC_4H_8)_3$, 66758-43-8; $Ta_2Br_6(SC_4H_8)_3$, 65651-12-9; $Nb_2Cl_6(SC_4H_8)_3$, 38531-73-6; $Nb_2Br_6(SC_4H_8)_3$, 38531-74-7; $Nb_2I_6(SC_4H_8)_3$, 38585-03-4.

References and Notes

(1) D. Brown in "Comprehensive Inorganic Chemistry", Vol. 3, Pergamon Press, Rushcutters Bay, Australia, 1973, pp 553–622.
(2) H. Schäfer, R. Gerken, and H. Scholz, *Z. Anorg. Allg. Chem.*, **335**, 96 (1965).
(3) R. C. Mehrotra, A. K. Rai, P. N. Kapoor, and R. Bohra, *Inorg. Chim. Acta*, **16**, 237 (1976).
(4) D. A. Miller and R. D. Bereman, *Coord. Chem. Rev.*, **9**, 107 (1972).
(5) D. G. Blight, R. L. Deutscher, and D. L. Kepert, *J. Chem. Soc., Dalton Trans.*, 87 (1972).
(6) P. A. Finn, M. S. King, P. A. Kilty, and R. E. McCarley, *J. Am. Chem. Soc.*, **97**, 220 (1975).
(7) E. T. Maas, Jr., and R. E. McCarley, *Inorg. Chem.*, **12**, 1096 (1973).
(8) J. L. Templeton, W. C. Dorman, J. C. Clardy, and R. E. McCarley, *Inorg. Chem.*, in press.
(9) F. A. Cotton and D. A. Ucko, *Inorg. Chim. Acta*, **6**, 161 (1972).
(10) R. E. McCarley, B. G. Hughes, J. C. Boatman, and B. A. Torp, *Adv. Chem. Ser.*, **No. 37**, 243 (1963).
(11) J. G. Converse and R. E. McCarley, *Inorg. Chem.*, **9**, 1361 (1970).
(12) P. A. Edwards, Ph.D. Thesis, Iowa State University of Science and Technology, Ames, Iowa, 1972.
(13) P. A. Edwards, R. E. McCarley, and D. R. Torgeson, *Inorg. Chem.*, **11**, 1185 (1972).
(14) P. W. Selwood, "Magnetochemistry", 2nd ed, Interscience, New York, N.Y., 1956.
(15) J. Lewis, J. R. Miller, R. L. Richards, and A. Thompson, *J. Chem. Soc.*, 5850 (1965).
(16) J. B. Hamilton and R. E. McCarley, *Inorg. Chem.*, **9**, 1333 (1970).
(17) S. L. Segel and R. G. Barnes, *USAEC Rep.*, **IS 520** (revised) (1968).
(18) E. A. C. Lucken, "Nuclear Quadrupole Coupling Constants", Academic Press, New York, N.Y., 1969.
(19) T. L. Brown, W. G. McDugle, Jr., and L. G. Kent, *J. Am. Chem. Soc.*, **92**, 3645 (1970).
(20) G. K. Semin, S. I. Kuznetsov, I. M. Alimov, T. L. Khotsianova, E. V. Bryukhova, L. A. Nisselson, and K. V. Tretyakova, *Inorg. Chim. Acta*, **13**, 181 (1974).
(21) For the bridging halogen atoms the electric field gradient tensor is best discussed with the coordinates chosen so that the *X* and *Y* axes lie in the M–X–M plane and project over the M–X bridge bonds, and the *Z* axis is perpendicular to the M–X–M plane. With this choice of axes it will be the halogen p_x and p_y orbitals which enter into σ bonding with the metal, while the p_z orbital will be unaffected and populated with a nonbonding electron pair. For the terminal halogens the *Z* axis is chosen to be coincident with the M–X bond axis and hence only the p_z orbital enters into σ bonding.
(22) C. B. Harris, *Inorg. Chem.*, **7**, 1517 (1968), and references therein.
(23) P. A. Edwards and R. E. McCarley, *Inorg. Chem.*, **12**, 900 (1973).
(24) J. B. Hamilton, Ph.D. Thesis, Iowa State University of Science and Technology, Ames, Iowa, 1968.
(25) E. T. Mass, Jr., Ph.D. Thesis, Iowa State University of Science and Technology, Ames, Iowa, 1972.